A mineralogical and structural study of red corundum, $Al_{1.98}Cr_{.02}O_3$, from Froland, Norway

BENYAM ESTIFANOS, KENNY STÅHL, PER-GUNNAR ANDRÉASSON, GÖRAN BYLUND & LEIF JOHANSSON

Estifanos, B., Ståhl, K., Andréasson, P. G., Bylund, G. & Johansson, L.: A mineralogical and structural study of red corundum, $Al_{1.98}Cr_{.02}O_3$, from Froland, Norway. *Norsk Geologisk Tidsskrift*, Vol. 77, pp. 119–122. Oslo 1997. ISSN 0029-196X.

In this study, the red corundum, $Al_{1.98}Cr_{.02}O_3$, from Froland is characterized structurally and compositionally. The crystal structure has been refined from X-ray ($CuK\alpha_1$) powder diffraction data. Space group R $\bar{3}$ c Z = 6, a = 4.7597(4) Å, c = 13.0013(9) Å. The substituting Cr-atoms do not take the site of Al-atoms, they depart 1.04 Å in the direction of the vacant octahedral interstices. A SEM (EDS) study revealed microphases of diaspore; one of the reasons for gem quality being lost. The result suggests that the reaction Al_2O_3 (Crn) + $H_2O \Leftrightarrow$ 2AlO(OH) (Dsp) occurred in the late stage of the metamorphic history of the Froland region.

B. Estifanos, P. G. Andréasson, G. Bylund & L. Johansson, Department of Geology, University of Lund, Sölvegatan 13, S-223 62 Lund, Sweden; K. Ståhl, Inorganic Chemistry 2, University of Lund, P.O. Box 124, S-221 00 Lund, Sweden.

Introduction

Corundum from the occurrence at Froland (Norway) is known for its deep red colour, large crystal size, fracture pattern, and poor quality in relation to gem standard (Oftedahl 1963). Oftedahl (1963) studied the Froland corundum in thin sections and described features such as fracturing, zoning and inclusions, microperthite structures, parting and lamellar twinning. Based on the study of the Froland corundum-bearing rocks, Nijland et al. (1993) constrained the cooling and uplift history of the Bamble Sector (South Norway). This work has closely observed the role of foreign atom substitutions and inclusions in the formation and paragenesis of red corundum.

Corundum (α-Al_2O_3) is a rock-forming mineral in igneous and metamorphic rocks. The corundum structure was first refined by Pauling & Hendricks (1925). Corundum is trigonal with space group R $\bar{3}$ *c*. Since the introduction of the Rietveld method (Rietveld 1969), α-Al_2O_3 has furthermore been studied intensively (Thompson et al. 1987; Hill & Madsen 1991; Brown et al. 1993).

Pure alumina is neither phosphorescent nor fluorescent; however, the presence of 0.0001% chromic oxide induces a distinct fluorescence (Werfers & Bell 1972). Red corundum of gem quality is called ruby. The single crystal refinement of ruby (0.46 wt% Cr) by Tsirelson et al. (1985) showed that the Cr-atoms do not substitute precisely for the Al-atoms at the sites.

Powder diffraction refinements

A powder diffraction pattern was collected with an INEL powder diffractometer, equipped with a CPS120 position sensitive detector covering 120° in 2θ, and using $CuK\alpha_1$ radiation (Ståhl & Thomasson 1992).

The Rietveld analysis[1] program used in this work is essentially the RIETAN-94 program (Izumi 1993) adopted to fit the local experimental conditions. An asymmetric (Howard 1982) and modified pseudo-Voigt profile-shape function (Thompson et al. 1987) is used to fit recorded intensities. The angular range is set between $24° < 2\theta < 115°$. The starting lattice parameters of corundum, rutile, and quartz are given by Tsirelson et al. (1985), Newnham & Haan (1962), and Ståhl & Thomasson (1992) respectively.

Final residual values were $R_p = 8.87\%$, $R_{wp} = 11.49\%$, and $R_B = 5.32\%$ from 2974 observations, and 37 refined parameters. Structural parameters are given in Tables 1 and 2. The observed diffraction pattern and the final difference pattern are shown in Fig. 1.

The first task was to determine the site of the chromium atom in the corundum phase. In red corundum, Cr-atoms depart 1.04 Å from Al-atoms in the direction of the vacant octahedral interstices. The Cr–Cr distance is short ($\approx$1.7 Å). Within this range one chromium is sited. Chromium could be coordinated to six oxygens in a distorted trigonal prism. The raw pattern in Fig. 1 reveals extra phases. The presence of böhmite (Bhm), diaspore (Dsp), gibbsite (Gbs), kyanite (Ky), muscovite (Ms($2M_1$,3T)), orthoclase (Or), quartz (Qtz), rutile (Rt), sillimanite (Sil) was tested. Subtraction of rutile and quartz yielded better residuals. The calculated mass fractions (Hill & Howard 1987) of the three phases are 95.82% (Crn), 1.61% (Rt), and 2.56% (Qtz). Isolated grains of quartz were not observed. However, the corundum (Dsp) along the corundum ($\pm$Dsp)/alu-

[1] A complete list of refined parameters and step intensity data is held by the first author.

Table 1. Fractional coordinates, anisotropic temperature factors (*10^6), isotropic temperature factor coefficient, and occupancies for red corundum.

	x/a	y/b	z/c	B [Å^2]/β_{ij}	g
Al	0	0	0.3515 (7)	β_{11} 3562	0.9901
				β_{33} 377	
Cr	0	0	0.43 (4)	β_{iso} 2.61	0.0099
O	0.3028 (23)	0	0.2500	β_{11} 289	1.0
				β_{22} 265	
				β_{33} 27	
				β_{13} 50	

Table 2. The unit cell parameters [Å] and distances [Å] in red corundum. Distances are calculated using ORFEE (Busing et al. 1964).

a	4.7597 (4)		
c	13.0013 (9)		
Al–Cr	1.043 (78)	Cr–Cr	1.775 (109)
Al–3O	1.867 (5)	Cr–3O	1.675 (66)
Al–3O	1.954 (8)	Cr–3O	2.579 (42)
Al–Al	2.640 (19)		
Al–3Al	2.788 (3)		
O–2O	2.496 (19)		
O–2O	2.614 (4)		
O–4O	2.732 (3)		
O–4O	2.881 (11)		

minium silicate interface and along some cracks contains SiO_2 (1.0–5.3 wt%). Quartz is probably the product of the late-stage alteration of aluminium silicates.

Electron probe micro studies

Compositional and image analysis were performed using JEOL JSM-6400 SEM equipped with Ge solid detector. ZAF correction was conducted using LINK/LEMSAS programs. Operating conditions were 18 keV and 60 nA.

Numerous works have contributed to the knowledge of the stability relations of minerals in the system Al_2O_3-H_2O (Ervin & Osborn 1951; Althaus 1969; Werfers & Bell 1972; Voigt et al. 1977; Perkins et al. 1979; Hemley et al. 1980; Chesworth et al. 1994). An electron probe micro study was performed on the same corundum-bearing sample. Figure 2 testifies to the formation of diaspore (Table 3). The Cr_2O_3 content is lower (0.78 wt%). However, foreign ions could stabilize the formation of diaspore (Gore & Verdes 1993). Figure 3a shows diaspore seams confirmed to fractures and parting planes along the diaspore/corundum interface. This alteration is one of the reasons for gem quality being lost. Figure 3b is an inset from Fig. 3a revealing corundum, diaspore, a metastable phase (Dsp2), muscovite, and poorly crystallized illite. Nijland et al. (1993) reported that plagioclase, biotite and aluminium silicate are locally altered to sericite/muscovite ± calcite. A rim of diaspore is usually present around both mica and calcite inclusions. Illite probably formed from hydrothermally altered muscovite or relics of feldspar. Diaspore, böhmite, and gibbsite contain on average 85 wt%, 80 wt%, and 65 wt% Al_2O_3 respectively. The region Dsp2 in Fig. 3b with 73 wt% Al_2O_3 could be a metastable phase of böhmite/gibbsite or a fine mixture of the three phases. The region in Fig. 4 (Crn_{ss}) has an average composition of (Table 3) 5–6 wt% TiO_2 and 1.5–2 wt% SiO_2. It is, in optical microscopy, indistinguishable from corundum. The Crn_{ss} may contain rutile and quartz as impurities. Rutile needles are also observed. Quartz probably exists in solid solution.

Conclusions

The Rietveld analysis of red corundum shows that the substituting Cr-atoms are positioned in the vacant octahedral interstices. This Cr-ion ordering stabilizes the transition to diaspore. The presence of rutile and quartz is also revealed. The content of foreign atoms strongly affects the crystal's physical character (colour, parting).

In the late-stage cooling and uplift history of the Froland area, the reaction of red corundum with water introduced diaspore and possibly metastable aluminium

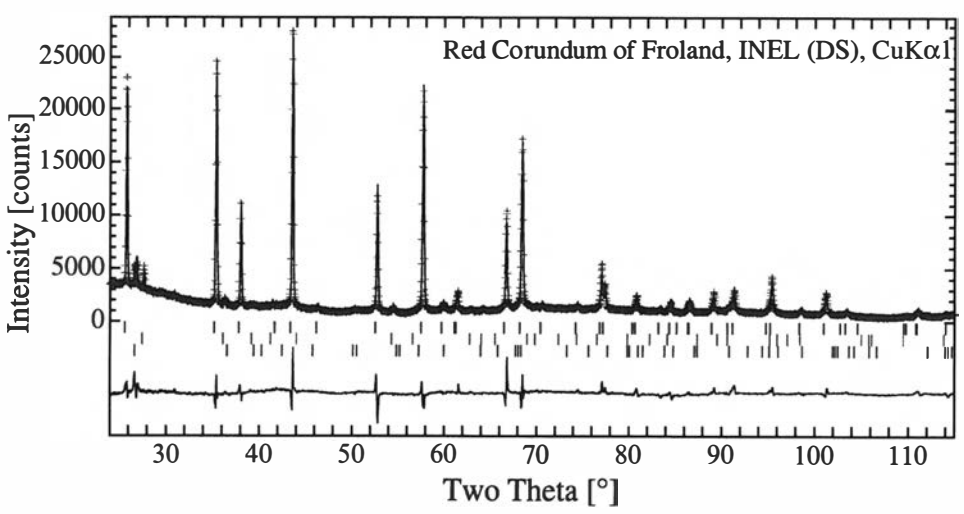

Fig. 1. Rietveld refinement plot for red corundum. The upper curve is the observed and calculated pattern. The lower curve is the difference between the observed and the calculated intensity. The upper, medium, and lower rows of tick marks correspond to the positions of all possible reflections of red corundum, rutile and quartz respectively.

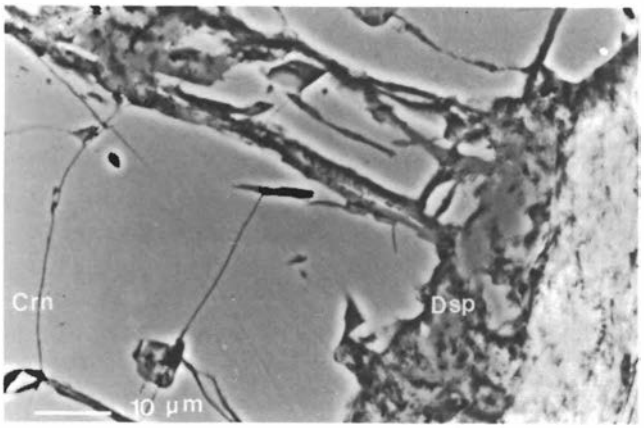

Fig. 2. SEM (back-scattered electron) images of partially transformed red corundum (Crn) and diaspore (Dsp). Mineral symbols according to Kretz (1983).

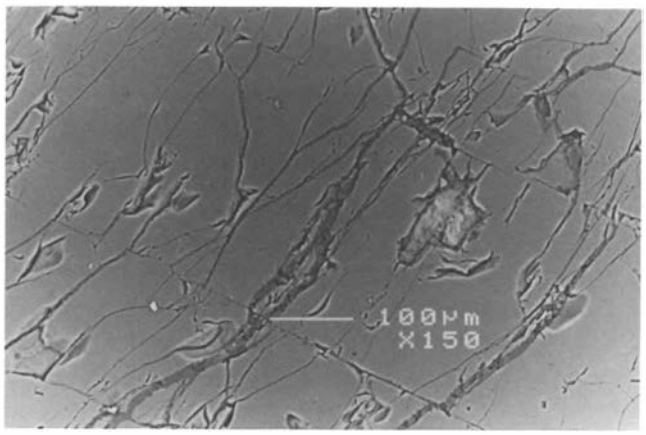

Fig. 3a. SEM (back-scattered electron) images showing the web of diaspore seams in red corundum.

oxide hydroxide and trihydroxides. The P-T equilibrium between diaspore and corundum could exceed 7.5 kbar/460°C (Haas 1972). Nijland et al. (1993) reconstructed the P-T path during exhumation and cooling of the Froland corundum-bearing rocks and identified five stages. Since they did not observe any diaspore, they concluded that the reaction Crn + water = Dsp did not occur, but used the reaction line as an upper limit of P-T conditions during the fourth stage (Fig. 5). They reported coexisting kyanite and andalusite during the same stage. Our result suggests that the reaction Al_2O_3 (Crn) + $H_2O \Leftrightarrow$ 2 AlO(OH) (Dsp) actually occurred in

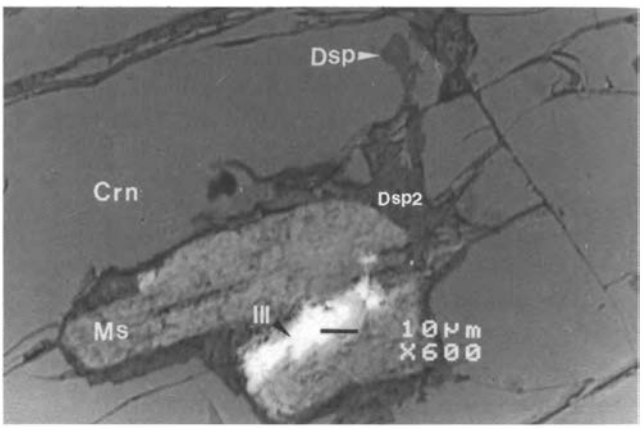

Fig. 3b. SEM (back-scattered electron) magnified images of a region from Fig. 3a revealing alteration products of diaspore (Dsp), metastable phase (Dsp2), muscovite (Ms), and illite (Ill).

Table 3. Average electron probe micro analyses of minerals shown in Figs. 2–4. Crn normalized to O = 3, Dsp to O = 2, and Ms, Ill to O = 22. In Fig. 2 only Al and Cr are analysed.

	Fig. 2		Fig. 3b					Fig. 4
Phase	Crn	Dsp	Crn	Dsp	Dsp2	Ms	Ill	Crn_{ss}
Al_2O_3	98.08	85.61	98.54	83.38	73.15	36.58	27.77	88.92
Cr_2O_3	1.12	0.78	1.16	0.95	1.04	0.57	0.39	1.03
SiO_2	—	—	0.09	0.12	0.14	45.23	33.53	1.67
Na_2O	—	—	0.17	0.18	0.16	1.86	0.96	0.28
MgO	—	—	—	—	—	0.43	0.2	—
K_2O	—	—	—	0.01	0.01	7.79	3.83	0.11
CaO	—	—	0.01	—	—	0.01	0.06	0.09
TiO_2	—	—	—	—	0.03	0.75	0.25	5.70
V_2O_3	—	—	—	—	—	—	—	0.07
MnO	—	—	0.03	0.04	—	—	0.05	—
FeO	—	—	0.19	0.15	0.10	0.55	0.34	0.22
Total	99.20	86.39	100.19	84.68	74.63	93.77	67.38	98.09
Ions								
Al	1.98	1.32	1.98	1.32	1.32	5.75	5.94	1.84
Cr	0.02	0.01	0.02	0.01	0.01	0.06	0.05	0.01
Si	—	—	—	—	—	6.03	6.09	0.03
Na	—	—	—	0.01	—	0.48	0.33	0.01
Mg	—	—	—	—	—	0.08	0.05	—
K	—	—	—	—	—	1.32	0.89	—
Ca	—	—	—	—	—	—	0.01	—
Ti	—	—	—	—	—	0.07	0.03	0.08
V	—	—	—	—	—	—	—	—
Mn	—	—	—	—	—	—	—	—
Fe	—	—	—	—	—	0.06	0.05	—

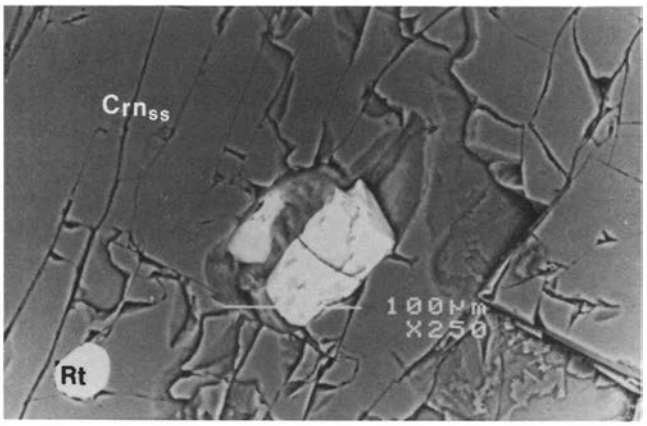

Fig. 4. SEM (back-scattered electron) images of rutile (Rt) needles and matrix (Crn_{ss}) in red corundum.

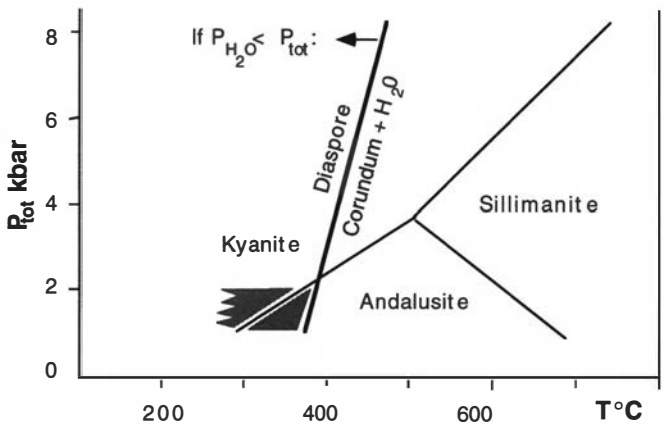

Fig. 5. Stability relationships of corundum and diaspore (Haas 1972). Alumina silicate triple point after Holdaway (1971). As deduced from results of this study and from observations of Nijland et al. (1993), the P-T path of the cooling Froland rocks passed through the shaded area of the diagram.

the late stage of the metamorphic history of Froland. This indicates that the P-T path of the Froland rocks passed through the shaded area in Fig. 5, suggesting pressures below 2 kbar during the fourth stage of cooling.

Acknowledgements. – This research was supported with grants from the Swedish Natural Science Research Council. Gilberto Artioli, Gunnar Raade, and two anonymous referees kindly read an early version of the manuscript. Thanks are extended to Iris and Carl Hugo, Takeshi Miyazu, and Tore Torngren for their invaluable co-operation.

Manuscript received April 1996

References

Althaus, E. 1969: Das System Al_2O_3-SiO_2-H_2O; experimentelle Untersuchungen und Folgerungen für die Petrogenese der metamorphen Gasteine; Teil III, Petrogenetische Folgerungen aus den Stabilitaetsbeziehungen der Al_2SiO_5-Modifikationen. *Neues Jahrbuch für Mineralogie Abhandlungen 111*, 144–161.

Brown, A. S., Spackman, M. A. & Hill, R. J. 1993: The electron distribution in corundum – a study of the uility of merging single-crystal and powder diffraction data. *Acta Crystallographia A49*, 513–527.

Busing, W. R., Martin, K. O. & Levy, H. A. 1964: A FORTRAN crystallographic function and error program, No. ORNL-TM-306, Oak Ridge National Laboratory.

Chesworth, W., Essene, W. J., Anovitz, L. M. & Perkins, D. 1994: Mineral metastability in the system Al_2O_3-SiO_2-H_2O; discussion and reply. *Clays & Clay Minerals 42*, 98–105.

Ervin, G. J. & Osborn, E. F. 1951: The system Al_2O_3-H_2O. *Journal of Geology 59*, 381–394.

Gout, R. & Verdes, G. 1993: Effect of crystallinity on diaspore and boehmite relative stability. *European Journal of Mineralogy* 5, 215–217.

Haas, H. 1972: Diaspore-corundum equilibrium determined by epitaxis of diaspore on corundum. *American Mineralogist 57*, 1375–1385.

Hemley, J. J., Montoya, J. W., Marinenko, J. W. & Luce, R. W. 1980: Equilibria in the system Al_2O_3-SiO_2-H_2O and some general implications for alteration/mineralization processes. *Economic Geology 74*, 210–228.

Hill, R. J. & Howard, C. J. 1987: Quantitatibe phase analysis from neutron powder diffraction data using the Rietveld method. *Journal of Applied Crystallography 20*, 467–474.

Hill, R. J. & Madsen, I. C. 1991: Rietveld analysis using para-focusing and Debye-Scherrer geometry data collected with a Bragg-Brentano diffractometer. *Zeitschrift für Kristallographie 196*, 73–92.

Holdaway, M. J. 1971: Stability of andalusite and the aluminium silicate phase diagram. *American Journal of Science 271*, 97–131.

Howard, C. J. 1982: The approximation of asymmetric neutron powder diffraction peaks by sums of gaussians. *Journal of Applied Crystallography 15*, 615–620.

Izumi, F. 1993: Rietveld analysis progrms RIETAN and PREMOS and special applications. *In* Young, R. A. (ed.): *The Rietveld Method*, 236–253. Oxford University Press, Oxford.

Kretz, R. 1983: Symbols for rock-forming minerals. *American Mineralogist 68*, 277–279.

Newnham, R. E. & Haan, Y. M. D. 1962: Refinement of the αAl_2O_3, Ti_2O_3, V_2O_3 and Cr_2O_3 structures. *Zeitschrift für Kristallographie 117*, 235–237.

Nijland, T. G., Liauw, F., Visser, D., Maijer, C. & Senior, A. 1993: Metamorphic petrology of the Froland corundum-bearing rocks: the cooling and uplift history of the Bamble Sector, South Norway. *Norges geologiske undersøkelse Bulletin 424*, 51–63.

Oftedahl, C. 1963: Red corundum of Froland at Arendal. *Norsk Geologisk Tidsskrift 43*, 431–440.

Pauling, L. & Hendricks, S. B. 1925: The crystal structures of hematite and corundum. *Journal of American Chemical Society 47*, 781–790.

Perkins, D., III, Essene, E. J., Westrum, E. F. J., Wall, V. J. & Hemley J. J. 1979: New thermodynamic data for diaspore and their application to the system Al_2O_3-SiO_2-H_2O solubilities in the system Al_2O_3-SiO_2-H_2O. *American Mineralogist 64*, 1080–1090.

Rietveld, H. M. 1969: A profile refinement method for nuclear and magnetic structures. *Journal of Applied Crystallography 2*. 65–71.

Ståhl, K. & Thomasson, R. 1992: Using cps 120 curved position-sensitive detector covering 120° powder diffraction data in Rietveld analysis. The dehydration process in the zeolite thomsonite. *Journal of Applied Crystallography 25*, 251–258.

Thompson, P., Cox, D. E. & Hastings, J. B. 1987: Rietveld refinement of Debye-Scherrer synchrotron x-ray data from Al_2O_3. *Journal of Applied Crystallography 20*, 79–83.

Tsirelson. V. G., Antipin, M. Y., Gerr, R. G., Ozerov, R. P. & Struchkov. Y. T. 1985: Ruby structure peculiarities derived from X-ray diffraction data. *Physica Status Solidi A87*, 425–433.

Voigt, R., Seifert, K. & Neuhaus, A. 1977: Ein Beitrag zum System Al_2O_3-H_2O unter hohen Drücken. *Neues Jahrbuch für Mineralogie-Monatshefte 5*, 238–240.

Werfers, K. & Bell, G. M. 1972: Oxides and hydroxides of aluminum. No. 19. Alcoa Research Laboratories.